


Impact of gas ultrafine bubbles on the efficacy of antimicrobials for eliminating fresh and aged *Listeria monocytogenes* biofilms on dairy processing surfaces

Phoebe Unger | Amninder Singh Sekhon | Sonali Sharma | Alexander Lampien | Minto Michael 

School of Food Science, Washington State University, Pullman, Washington, USA

Correspondence

Minto Michael, School of Food Science, Washington State University, Pullman, WA 99164, USA.
Email: minto.michael@wsu.edu

Funding information

BUILD Dairy program of the Western Dairy Center

Abstract

Ultrafine bubbles (UFB) are a novel concept that has the potential to enhance the potency of antimicrobials to eliminate biofilms. This study investigated the impact of incorporating gas (air, CO₂, and N₂) UFB on the potency of chlorine (Cl₂; 50, 100, and 200 ppm) and peracetic acid (PAA; 20, 40, and 80 ppm) antimicrobial (AM) solutions against fresh (3 days) and aged (30 days) *Listeria monocytogenes* biofilms on polypropylene, silicone, and stainless steel surfaces. *Listeria monocytogenes* biofilms were statically grown on polypropylene, silicone, and stainless steel coupons (7.62 × 2.54 cm) at 25°C for 3 or 30 days, by immersing in a three-strain cocktail of *L. monocytogenes* in brain heart infusion (BHI) broth. The coupons were treated by submerging in AM solutions with or without UFB for 1 min, then swabbed into Dey-Engley neutralizing broth and enumerated on BHI agar. Incorporation of air, CO₂, and N₂ UFB in AM solutions resulted in significantly increased log reductions (0.4–1.5 logs) of fresh and aged *L. monocytogenes* biofilms on polypropylene and stainless steel surfaces, whereas incorporation of CO₂ UFB in AM solutions resulted in ~1 log greater reductions of fresh and aged *L. monocytogenes* biofilms on silicone surfaces compared with AM solutions without UFB. This study also demonstrated that 200 ppm Cl₂ was most effective against fresh and aged *L. monocytogenes* biofilms on polypropylene, silicone, and stainless steel surfaces compared with 50 ppm Cl₂, 20 ppm PAA, and 40 ppm PAA.

1 | INTRODUCTION

Listeria monocytogenes is a gram-positive rod (0.5–4 μm in diameter and 0.5–2 μm in length), nonspore forming, facultative anaerobic bacteria (Osek et al., 2022). It is a ubiquitous bacterium that can be found in moist environments, soil, water, animals, and can survive and even grow under refrigeration (FDA, 2022). According to the Centers for Disease Control (CDC), an estimated 1600 people get listeriosis, an infection

usually caused by the consumption of eating contaminated food with *L. monocytogenes*, and roughly 260 die each year in the United States (CDC, 2022a; Scallan et al., 2011). Elderly, pregnant women, newborns, and individuals with weakened immune systems are most severely affected by the disease (CDC, 2022a, 2022b), and common clinical consequences of listeriosis include but are not limited to; sepsis, meningitis, endocarditis, septicemia, brain infection, miscarriage, and stillbirth (Matle et al., 2020). The success of *L. monocytogenes* to induce infection

This is an open access article under the terms of the [Creative Commons Attribution](https://creativecommons.org/licenses/by/4.0/) License, which permits use, distribution and reproduction in any medium, provided the original work is properly cited.

© 2023 The Authors. *Journal of Food Safety* published by Wiley Periodicals LLC.

is due to its ability to internalize through the host cell (Carvalho et al., 2014). The process of infection in host cell involves several different stages; adhesion and invasion of host cell, internalization by the host cell, lysis of vacuole, intercellular multiplication, and intercellular spread to adjacent cells (Chen et al., 2009).

Past outbreaks of *L. monocytogenes* have been linked to raw, unpasteurized milks and cheeses, ice cream, vegetables, fruits, raw and undercooked poultry, sausages, hotdogs, delicatessens, seafood, and even pet food (CDC, 2022b, FDA, 2022). According to the CDC, since 2012, 13 of the 17 reported outbreaks of *L. monocytogenes* have been from dairy products, such as cheese, milk, and ice cream (CDC, 2022b). Due to their high prevalence, ensuring the safety of dairy products by eliminating this foodborne pathogen is vital in the dairy industry.

Listeria monocytogenes can contaminate raw milk on the farm through milking animals, farm workers, and the farm environment, but *L. monocytogenes* is killed during pasteurization. However, postpasteurization recontamination can occur in dairy products through workers and processing environment (Bourdichon et al., 2019). *Listeria monocytogenes* is frequently found in moist areas, including drains, floors, coolers, conveyors, and washing areas of food processing facilities (Cornell University, 2008). So, it is vital for dairy processing facilities to have well-established sanitation procedures to control foodborne pathogens; however, some foodborne pathogens, such as *L. monocytogenes*, have the ability to form biofilms and present an additional hurdle in sanitation.

A biofilm is defined as an aggregate of microorganisms in which cells that are embedded within a self-produced matrix of extracellular polymeric substance (EPS) adhere to each other and/or surface (Vert et al., 2012). The EPS, also referred to as slime, which is a polymeric conglomeration generally composed of polysaccharides, proteins, lipids, and extracellular DNA can protect bacteria against various foodborne pathogen control steps such as antimicrobial (AM) and heat treatments, and cleaning and sanitization processes (Bremer et al., 2015; Flemming & Wingender, 2010). Biofilms not only cause a hindrance during cleaning and sanitization resulting in microbial contamination, but they can also affect the process efficiency by restricting flow in equipment, reducing heat transfer in heat exchangers, and promoting surface corrosion on equipment (Bremer et al., 2015). Therefore, inhibition, disruption, and elimination of biofilms in dairy processing facilities are vital steps to ensure food safety.

Due to biofilms stubborn and persistent nature in the dairy industry, food scientists are continuously exploring novel technologies to help eliminate biofilms and further improve product safety. Ultrafine bubbles (UFB) technology is a novel concept that has the potential to enhance the potency of commonly used AMs in cleaning and sanitization. The UFB are defined by the International Organization for Standardization (ISO) as a gas in a medium enclosed by an interface with a volume equivalent diameter of $<1 \mu\text{m}$ (International Organization for Standardization (ISO), 2017). Therefore, the term nanobubbles was unified with UFB in 2017. The UFB technology is still new in the field of food safety; however, it is hypothesized to improve the potency of AMs against foodborne pathogens and biofilms. This improved AM potency with the incorporation of UFB is attributed to the increased

stability of the bubbles, larger surface area, negative zeta potential, the generation of free radicals in solutions, and better delivery of AMs (Agarwal et al., 2011; Ghadimkhani et al., 2016; Guo et al., 2019; Martirosyan et al., 2012; Sikin et al., 2017; Takahashi et al., 2021).

Despite being novel in the field of food safety, UFB have been effectively utilized in several other sectors such as agriculture (improved seed germination, plant growth, and wastewater treatment), fisheries (accelerated shellfish growth), and medicine (inhibition of tumor cells; Ahmed et al., 2018; Asada et al., 2010; Hayakumo et al., 2014; Liu et al., 2017; Liu, Oshita, Kawabata, et al., 2016; Liu, Oshita, Makino, et al., 2016; Owen et al., 2016).

The UFB can be made with any gas; however, in the field of food science carbon dioxide (CO_2), nitrogen (N_2), and ozone (O_3) are commonly studied (Khalesi et al., 2016; Phan et al., 2020). Multiple generation methods to create gas UFB can be used, but the most common techniques in UFB generation include venturi flow or cavitation type, pressurized dissolution type, swirl liquid flow type, and membrane type (Arumugam, 2015; Dhungana & Bhandari, 2021; Phan et al., 2021).

Minimal studies have been conducted on the use of UFB to eradicate or reduce biofilms to improve dairy products safety. It is hypothesized that the gas UFB could disrupt the physical structural integrity of biofilms, which could help eliminate the bacterial cells in the biofilms (Horejs, 2018). In previous research, we assessed the impact of gas UFB (referred as microbubbles–nanobubbles) on the efficacy of commonly used AMs in the food industry and demonstrated that the use of CO_2 UFB increased the potency of 200 ppm Cl_2 and 28.4 ppm PAA solutions against *Escherichia coli* O157: H7 and *L. monocytogenes* in growth media compared with these AM solutions without UFB (Singh et al., 2021). In another preliminary study, we evaluated the impact of UFB on the efficacy of AMs against fresh *L. monocytogenes* biofilms on stainless steel surfaces and revealed that the incorporation of air and CO_2 UFB in 100 ppm Cl_2 led to significantly greater log reductions in *L. monocytogenes* compared with 100 ppm Cl_2 without UFB (Sekhon et al., 2021). After proving the potency of AM in growth media and fresh *L. monocytogenes* biofilms could be improved by incorporating gas UFB, the next logical step was to evaluate the effectiveness of gas UFB against pathogenic biofilms (such as *L. monocytogenes*) on different dairy processing surfaces using more robust experimental design. Thus, the primary objective of this research was to investigate the impact of incorporating gas (air, CO_2 , and N_2) UFB on the potency of Cl_2 (50, 100 and 200 ppm) and PAA (20, 40 and 80 ppm) AM solutions against fresh and aged *L. monocytogenes* on polypropylene, silicone, and stainless steel surfaces.

2 | MATERIALS AND METHODS

2.1 | Culture propagation

Three strains of *L. monocytogenes* were acquired from the American Type Culture Collection (ATCC[®], Manassas, Virginia; ATCC 19111, ATCC 19115, and ATCC 5414). Propagated cultures were transferred individually onto glycerol protectant cryogenic beads (Microbank™,

Bacterial and Fungal Preservation System, Pro-lab Diagnostics, Round Rock, Texas) and stored in a -80°C freezer (Panasonic Healthcare Co., Ltd.; Wood Dale, Illinois). At the beginning of this research, individual beads of respective bacteria were transferred into 10 mL of brain heart infusion (BHI) broth (Difco, Becton, Dickinson and Company, Sparks, Maryland), incubated at 37°C for 24 h, and stored as stock culture at 4°C . Using API[®] *Lister* (bioMérieux, Inc., Durham, North Carolina) all stock cultures were confirmed as *L. monocytogenes*.

2.2 | Biofilm preparation

For each replication, 0.2 mL of each stock culture was individually transferred into 20 mL of BHI broth and incubated at 37°C for 24 h. Freshly grown cultures were mixed in equal proportions to obtain a master inoculum of a three-strain *L. monocytogenes* cocktail. Fresh biofilms were grown on polypropylene, silicone, and stainless steel (SS-304) coupons (7.62×2.54 cm) through static incubation at 25°C for 72 h by immersing vertically in 40 mL *L. monocytogenes* inoculated BHI broth inoculated with 1 mL of three-strain *L. monocytogenes* master inoculum (9.49 ± 0.04 log CFU/mL). During biofilm development, 20 mL of inoculated BHI broth was replaced by fresh BHI broth after 36 h of incubation.

Similarly, aged biofilms were grown on polypropylene, silicone, and stainless steel (SS-304) coupons (7.62×2.54 cm) through static incubation at 25°C for 30 days. During biofilm development, 20 mL of inoculated BHI broth was replaced by fresh BHI after every 5 days of incubation. After the 72 h or 30-day incubation period, the coupons were gently removed from inoculated BHI broth and placed vertically into sterile water for 30 s to remove the loosely adhered cells and excess broth. The coupons were then dried inside the biosafety cabinet for 5 min.

2.3 | UFB generation

In this study, a microbubble–nanobubble generator (LEA15; Living Energies & Co., Shizuoka, Japan) equipped with a pressure gauge, gas flow meter, liquid relief valve, gas relief valve, gas inlet pipe, outlet valve, and inlet and outlet hoses, was used to generate UFB (Singh et al., 2021). As per the certificate of analysis from the manufacturer, the mean size and concentration of bubbles measured using NANO-SIGHT (Nanoparticle Tracking Analysis) should be 163.9 ± 4.3 nm and $1.03 \times 10^9 \pm 2.01 \times 10^7$ particles/mL, respectively. The gas (CO_2 or N_2) UFB were generated using food-grade compressed cylinders of CO_2 or N_2 gas, and natural air from the laboratory was used to prepare air UFB. Briefly, UFB were generated in water by adjusting the solution outlet valve position at 58.01 psi on the pressure gauge, and the gas inlet flow rate to 0.6 L min^{-1} . The UFB generator was allowed to run for 5 min after the pressure at the outlet gauge reached 58.01 psi. During the experiment, the water solutions of various gas UFB were also sent to a third-party laboratory for confirming the presence of UFB and determine their mean size using NANO-SIGHT, and all samples were analyzed within 36 h. The mean size and concentration of the

UFB produced were 227.6 ± 3.4 nm and $3.41 \times 10^8 \pm 5.3 \times 10^7$ particles/mL, 213.9 ± 2.4 nm and $1.98 \times 10^8 \pm 2.2 \times 10^7$ particles/mL, and 228.4 ± 7.16 nm and $2.63 \times 10^8 \pm 5.8 \times 10^7$ particles/mL for air, CO_2 , and N_2 UFB, respectively.

2.4 | AM solution preparation

The AM solutions were prepared to attain 50, 100, and 200 ppm free Cl_2 , and 20, 40, and 80 ppm PAA using city water (with or without UFB). The different Cl_2 solutions were prepared using bleach (7.5% available Cl_2 ; The Clorox Company, Oakland, California); whereas, the PAA solutions were prepared using 35% PAA stock solutions (Pfaltz & Bauer, Waterbury, Connecticut). All solutions were prepared and used at ambient air temperature ($\sim 20^{\circ}\text{C}$). Respective solutions were individually transferred to sterile 50 mL centrifuge tubes (VWR International, Radnor, Pennsylvania) to be used for further testing AM activity against fresh and aged *L. monocytogenes* biofilms on polypropylene, silicone, and stainless steel coupons. The concentration of the Cl_2 and PAA solutions was confirmed using Cl_2 (AquaCheck, Loveland, Colorado) and PAA concentration test strips (Hydriion, Micro Essentia Laboratory Inc., Brooklyn, New York).

2.5 | AM treatment of biofilms

The biofilm-laden polypropylene, silicone, and stainless-steel coupons were immersed vertically in the respective AM solutions for 1 min. Following the respective treatments, individual coupons were swabbed with a sterilized cotton swab on one side (Puritan[®], Guilford, Maine), and the swab was transferred aseptically to a 10 mL of Dey-Engley (DE) neutralizing broth (Hardy Diagnostics, Santa Maria,

TABLE 1 The *p*-values of ultrafine bubble (UFB), antimicrobial (AM), and their interactions for the log reductions of *Listeria monocytogenes* (LM) in fresh polypropylene (Fresh-PP), fresh silicone (Fresh-S), fresh stainless steel (Fresh-SS), aged polypropylene (Aged-PP), aged silicone (Aged-S), aged stainless steel (Aged-SS) biofilms, and the Eh and pH of AM solutions.

Parameters	<i>p</i> -Value		
	UFB	AM	AM × UFB
LM fresh-PP	<0.001*	<0.001*	0.925
LM fresh-S	<0.001*	<0.001*	0.939
LM fresh-SS	0.005*	<0.001*	0.681
LM aged-PP	<0.001*	<0.001*	0.484
LM aged-S	<0.001*	<0.001*	0.762
LM aged-SS	<0.001*	<0.001*	0.992
Eh	<0.001*	<0.001*	<0.001*
pH	<0.001*	<0.001*	<0.001*

Note: UFB: air, carbon dioxide, and nitrogen, and no gas; AM: 20 ppm peracetic acid (PAA), 40 ppm PAA, 80 ppm PAA, 50 ppm Cl_2 , 100 ppm Cl_2 , and 200 ppm Cl_2 .

*Effects are significant if $p \leq 0.05$.

California), to neutralize the lethality effect of the AM solutions. This procedure was then repeated with a second swab on the same side, being transferred into the same 10 mL of DE neutralizing broth as the first swab. Samples were then vortexed for 1 min at 3,000 rpm. Untreated coupons also underwent the same swabbing procedure after rinsing in water and air drying for 5 min (but without any AM dip treatment) and were used to determine the initial untreated bacterial population of the biofilms on respective surfaces.

2.6 | Microbial analyses

Microbial populations of the biofilms on the coupon were enumerated on nutrient-rich agar. First, the samples of vortexed DE broth were serially diluted using 0.1% of peptone water (Difco™, Becton, Dickinson, and Company, Sparks, Maryland) and then plated in duplicates on BHI agar (Difco™, Becton, Dickinson, and Company, Sparks, Maryland). The agar plates were incubated at 37°C for 48 h and the

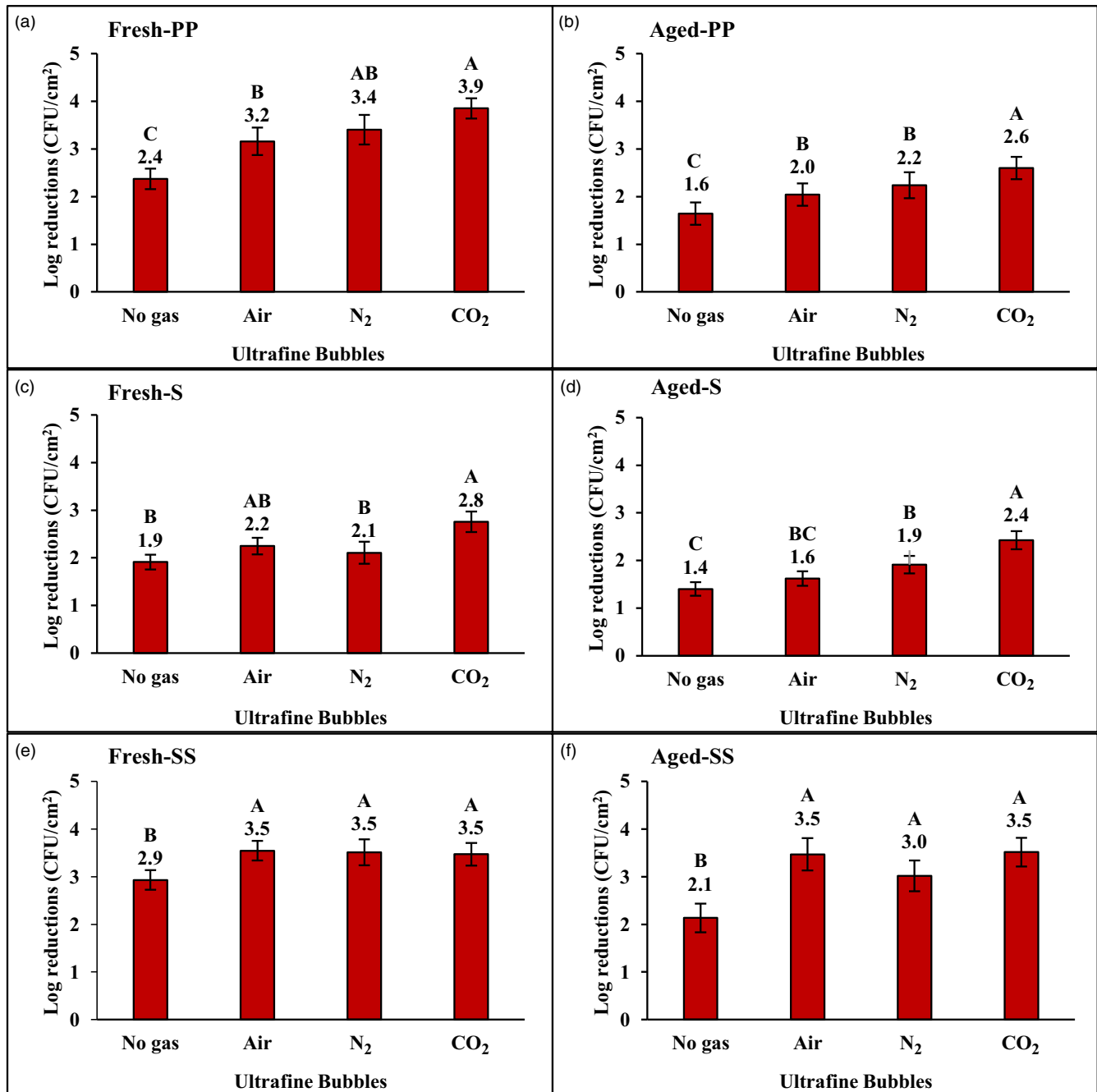


FIGURE 1 *Listeria monocytogenes* reductions (Log CFU/cm²) in (a) fresh biofilms on polypropylene (Fresh-PP), (b) aged biofilms on polypropylene (Aged-PP), (c) fresh biofilms on silicone (Fresh-S), (d) aged biofilms on silicone (Aged-S), (e) fresh biofilms on stainless steel (Fresh-SS), and (f) aged biofilms on stainless steel (Aged-SS) surfaces as a function of gas ultrafine bubbles [no gas, air, carbon dioxide (CO₂), and nitrogen (N₂)]. A–C: Bars are averaged for *L. monocytogenes* reductions for all antimicrobial treatments within respective ultrafine bubbles (mean ± SE, n = 18) and bars with different letters are significantly different (p ≤ 0.05).

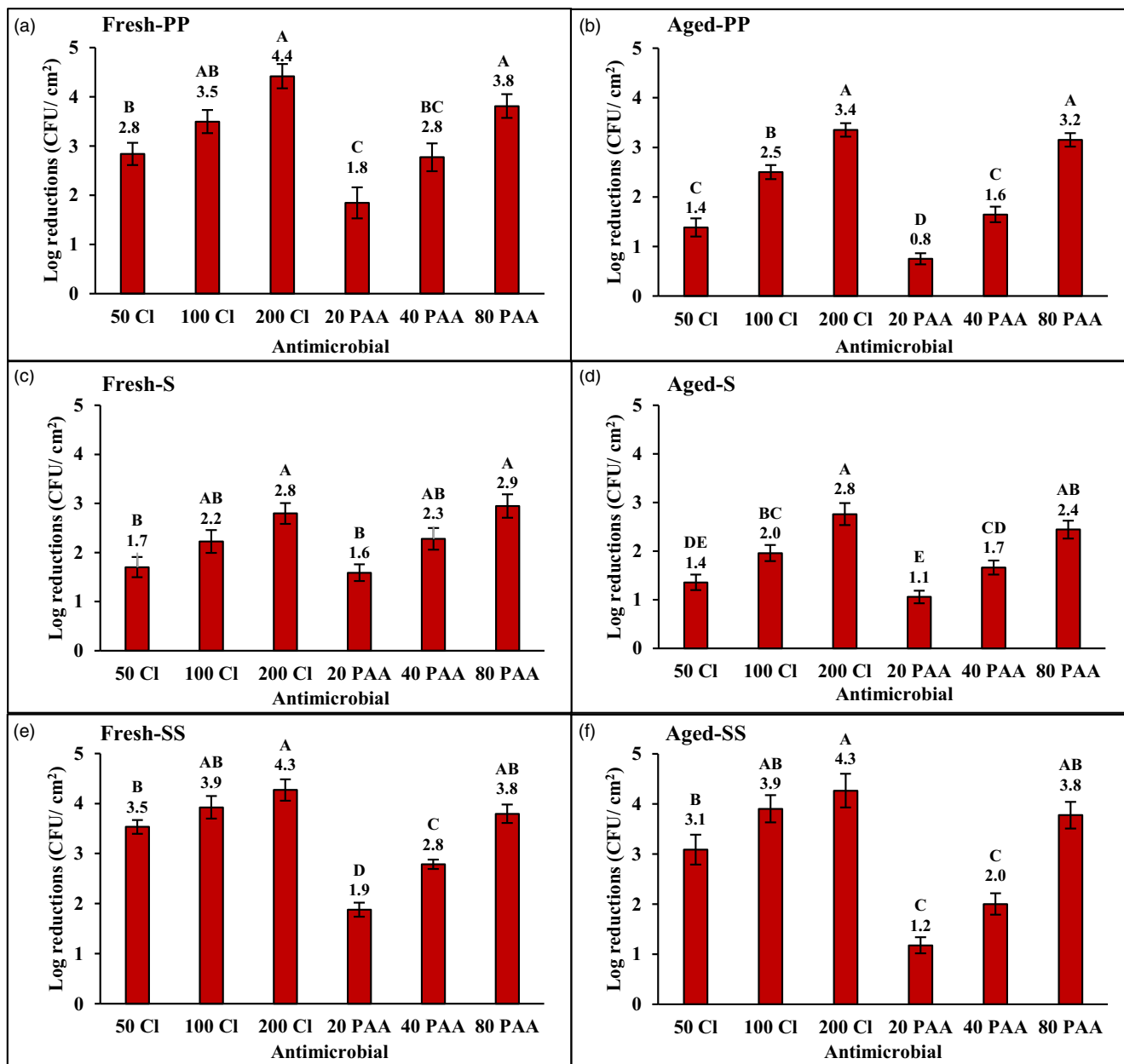


FIGURE 2 *Listeria monocytogenes* reductions (Log CFU/cm²) in (a) fresh biofilms on polypropylene (Fresh-PP), (b) aged biofilms on polypropylene (Aged-PP), (c) fresh biofilms on silicone (Fresh-S), (d) aged biofilms on silicone (Aged-S), (e) fresh biofilms on stainless steel (Fresh-SS), and (f) aged biofilms on stainless steel (Aged-SS) surfaces as a function of antimicrobial treatments (50 ppm chlorine [50 Cl], 100 ppm chlorine [100 Cl], 200 ppm chlorine [200 Cl], 20 ppm peracetic acid [20 PAA], 40 ppm peracetic acid [40 PAA], 80 ppm peracetic acid [80 PAA]). A–E: Bars are averaged for *L. monocytogenes* reductions for all types of ultrafine bubbles within respective antimicrobial treatment (mean ± SE, n = 12) and bars with different letters are significantly different (p ≤ 0.05).

bacterial colonies were counted. The log reductions (log CFU/cm²) for the respective treatments were calculated by subtracting the post-treatment biofilm bacterial population from the untreated biofilm bacterial population.

Biofilm log reductions (log CFU/cm²) = log CFU/cm² *L. monocytogenes* population on untreated biofilm - log CFU/cm² *L. monocytogenes* population posttreatment.

2.7 | pH and redox potential determination

The pH and Redox potential (Eh) of the AM solutions were measured at 25°C using calibrated pH and Eh meters. A Thermo Scientific™ Orion™ Eh meter (Thermo Fisher Scientific, Chelmsford, Massachusetts), and a Mettler Toledo™ pH meter (Mettler Toledo, Columbus, Ohio) were used for measuring Eh and pH, respectively.

2.8 | Experimental and statistical design

The fresh and aged, polypropylene, silicone, and stainless steel experiments were considered independent studies. Each study was designed as a two-factorial (4×6) randomized complete block design with three replications as blocks. The two factors were four gas types (air, CO₂, N₂, and no gas) and six AM (50 ppm Cl₂, 100 ppm Cl₂, 200 ppm Cl₂, 20 ppm PAA, 40 ppm PAA, and 80 ppm PAA). Within each replication, biofilms of *L. monocytogenes* were randomly treated with AM solutions (with or without UFB). Data were analyzed using two-way ANOVA, and Tukey's test was used to determine significant differences among the mean values at $p \leq 0.05$ using Minitab 19 (Minitab Inc., State College, Pennsylvania).

3 | RESULTS

The initial population of *L. monocytogenes* of the untreated fresh biofilms were 5.8 ± 0.22 , 5.4 ± 0.11 , and 5.3 ± 0.16 log CFU/cm² on polypropylene, silicone, and stainless steel surfaces, respectively. Similarly, the initial population of *L. monocytogenes* of the untreated aged biofilms were 5.5 ± 0.09 , 5.3 ± 0.07 , and 5.6 ± 0.11 log CFU/cm² on polypropylene, silicone, and stainless steel surfaces, respectively. Table 1 displays the p -values of the main effects (UFB and AM) and the interactions of the main effects for the microbial population

reductions of the *L. monocytogenes* biofilms, and the Eh, and pH of AM solutions.

The log reduction of *L. monocytogenes* biofilms on fresh and aged polypropylene, silicone, and stainless steel was all significantly affected by the UFB, and the AMs used in the study; however, they were not significantly impacted by the interaction of UFB and AMs (Table 1). The incorporation of air, CO₂, and N₂ UFB in various AM solutions resulted in significantly greater *L. monocytogenes* reductions in fresh and aged biofilms on polypropylene and stainless steel surfaces compared with solutions without UFB (Figure 1). Similarly, the incorporation of CO₂ UFB in AM solutions resulted in greater log reductions in *L. monocytogenes* fresh and aged biofilms on a silicone surface compared to solutions without UFB; however, the incorporation of air UFB resulted in similar log reductions on silicone surfaces as solutions without UFB (Figure 1).

The 200 ppm Cl₂ solution resulted in significantly greater log reductions in *L. monocytogenes* biofilms on fresh and aged polypropylene, silicone, and stainless steel surfaces compared with 50 ppm Cl₂, 20 ppm PAA, and 40 ppm PAA (Figure 2). The 20 ppm PAA solution resulted in the lowest log reduction of *L. monocytogenes* in fresh and aged biofilms on all surfaces (Figure 2). In general, the log reductions in the aged *L. monocytogenes* biofilms were less than or equal to the log reductions of fresh *L. monocytogenes* biofilms on all three surfaces when compared at the same AM concentration or UFB type (Figures 1 and 2).

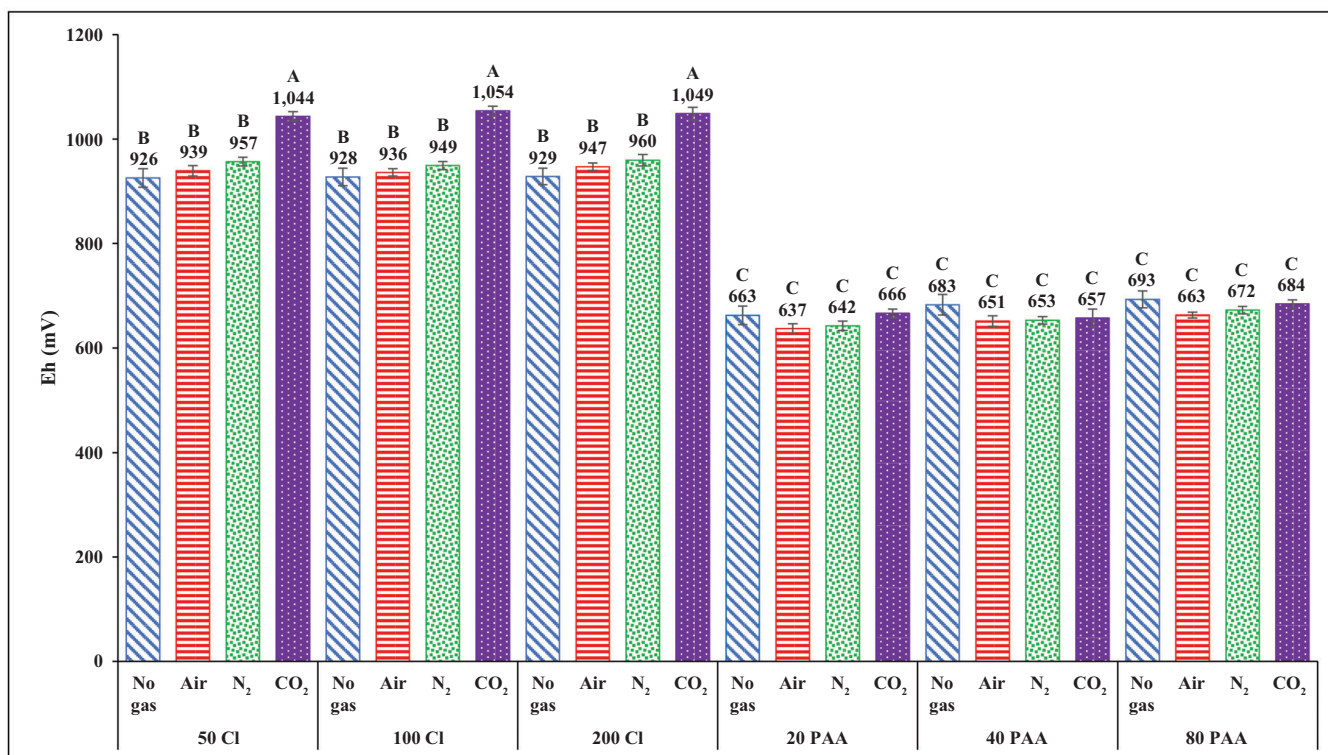


FIGURE 3 Redox potential (Eh) of antimicrobial solutions (50 ppm chlorine [50 Cl], 100 ppm chlorine [100 Cl], 200 ppm chlorine [200 Cl], 20 ppm peracetic acid [20 PAA], 40 ppm peracetic acid [40 PAA], and 80 ppm peracetic acid [80 PAA]) with or without gas ultrafine bubbles (no gas, air, carbon dioxide [CO₂], nitrogen [N₂]). A-C: Bars (mean \pm SE, $n = 18$) with different letters are significantly different ($p \leq 0.05$).

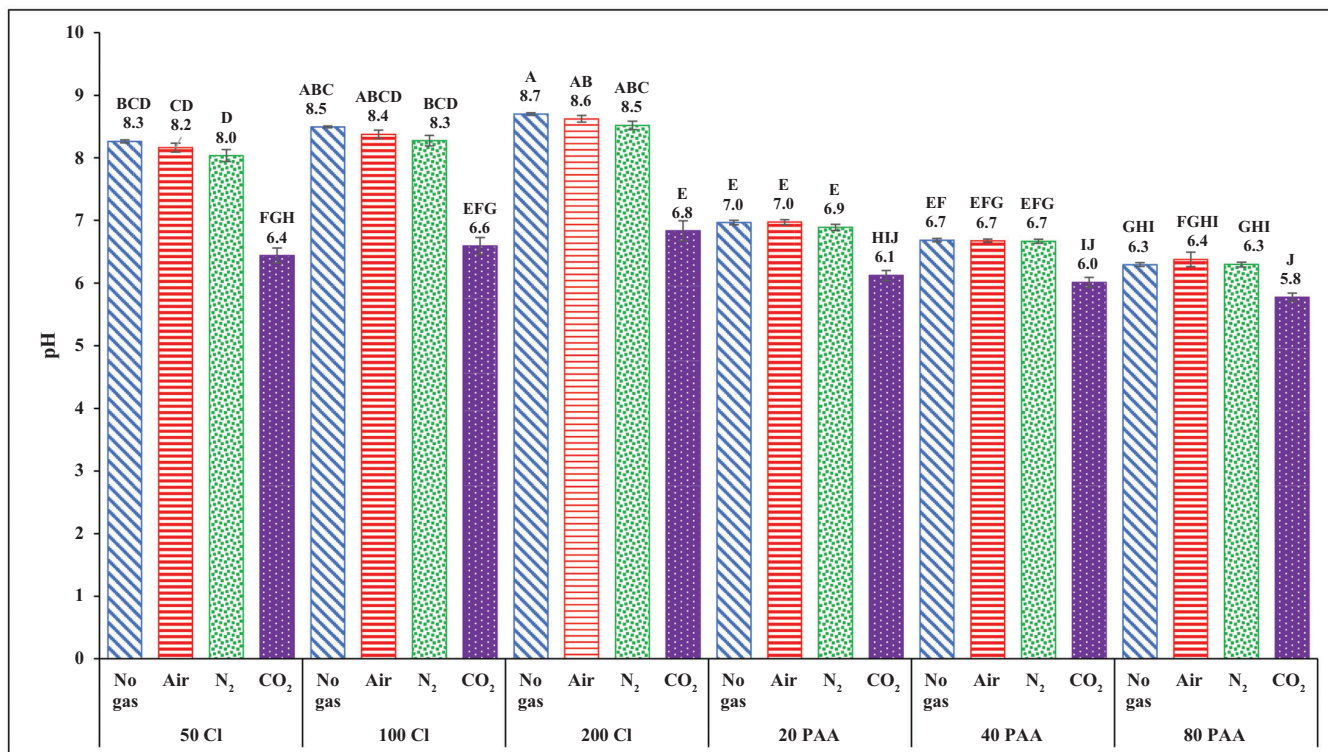


FIGURE 4 pH of antimicrobial solutions (50 ppm chlorine [50 chlorine [50 Cl], 100 ppm chlorine [100 Cl], 200 ppm chlorine [200 Cl], 20 ppm peracetic acid [20 PAA], 40 ppm peracetic acid [40 PAA], and 80 ppm peracetic acid [80 PAA]) with or without gas ultrafine bubbles (no gas, air, carbon dioxide (CO₂), nitrogen [N₂]). A–J: Bars (mean ± SE, n = 18) with different letters are significantly different (p ≤ 0.05).

The Eh and pH were not only significantly impacted by the effects of gas UFB and AMs, but also their interactions (Table 1). The Eh of city water used for preparing the AM solutions was 562 ± 28.2 mV; while the Eh of the water with air, CO₂ and N₂ was 616 ± 31.5, 646 ± 25.1, and 604 ± 40.6 mV, respectively (data not presented). The incorporation of CO₂ UFB in Cl₂ solutions resulted in a significantly greater Eh, compared with Cl₂ solutions with air and N₂ UFB, and without UFB (Figure 3). On the contrary, the incorporation of air, N₂, and CO₂ UFB in PAA solutions resulted in similar Eh to PAA solutions without UFB. The Eh of the Cl₂ solutions was significantly greater than the Eh of PAA solutions (Figure 3).

The pH of the city water used for preparing various AM solutions was 7.75 ± 0.03; whereas the pH of the city water in air, CO₂, and N₂ UFB was 7.67 ± 0.33, 6.24 ± 0.10, and 7.60 ± 0.08, respectively (data not presented). The pH of the AM solutions was affected by the UFB, AMs, and the interaction between UFB and AMs (Table 1). The AM solutions with CO₂ UFB had significantly lower pH than respective AM concentration solutions with air and N₂ UFB, and without UFB (Figure 4). The pH of the Cl₂ solutions was significantly greater than the pH of the PAA solutions within the respective UFB incorporation (Figure 4).

4 | DISCUSSION

It is important to first understand the structure of biofilms, to better understand the impact of UFB AM solutions on the elimination of

the biofilms. As stated previously, biofilms are embedded in an EPS, which is composed of polysaccharides, proteins, lipids, and nucleic acids as well as water-insoluble compounds such as cellulose and amyloids (Bremer et al., 2015; Flemming et al., 2021; Flemming & Wingender, 2010). The EPS is self-secreted and protective matrix that surrounds and immobilizes microbial cells, which can establish stable spatial interactions (Flemming et al., 2021). This EPS matrix strengthens the biofilm structurally and is responsible for the foundation of structured microbial communities within a biofilm with emergent properties that are distinctly different from individual planktonic cells, leading to the stubborn and persistent nature of the biofilm (Flemming et al., 2016). The cells improved tolerance to AMs is postulated to be from the binding of EPS to the AM compounds, physical inhibition of the diffusion of AM compounds by EPS, and the chemical reactions of AM compounds with components of the EPS matrix, all of which decrease the concentration of AM compounds reaching the microbial cells within the biofilm (Bremer et al., 2015; Thurnheer et al., 2003).

As discussed earlier, the enhanced potency of AMs with the incorporation of UFB is strongly related to the physical properties of the UFB; increased stability, negative zeta potential, large specific surface area, high gas dissolution rate, and generation of free radicals (Demangeat, 2015; Ghadimkhani et al., 2016; Liu et al., 2014; Ushikubo et al., 2010). The stability of UFB in solution is attributed to the Brownian motion, selective adsorption of anions at the gas–liquid interface, and the negative zeta potential (Takahashi, 2005; Ushikubo

et al., 2010). These phenomena inhibit accumulation and coalescence of UFB and reduce the internal pressure within the bubbles by decreasing surface tension, which ultimately lead to enhanced stability in solution (Phan et al., 2020).

The presence of reactive oxygen species such as hydroxyl radical ions ($\cdot\text{OH}$) has been confirmed in water by using a fluorescent probe by Liu, Oshita, Kawabata, et al. (2016) and Liu, Oshita, Makino, et al. (2016). Similarly, Agarwal et al. (2011) also established the presence of hydroxyl radical ions and shock waves due to collapse of microscopic bubbles with high oxidizing power. The presence of hydroxyl radicals is significant since they are one of the most reactive free radicals and can react aggressively with organic and inorganic molecules, including DNA, carbohydrates, lipids, and proteins, all of which are found in the EPS of biofilms (Tvrdá & Benko, 2020). Many scientists have demonstrated that these free radical ions were produced during UFB generation (Agarwal et al., 2011; Li et al., 2009; Liu et al., 2014; Takahashi et al., 2007; Takahashi et al., 2021). During the generation of UFB, macrobubbles and microbubbles are also produced; Takahashi et al. (2021) demonstrated that microbubbles shrink and collapse underwater within several minutes, leading to the generation of free radical such as hydroxyl radical ions. Similarly, Agarwal et al. (2011) confirmed the presence of hydroxyl radicals ions due to the collapse of microscopic bubbles with high oxidating power, which could be responsible for the promising AM capabilities of UFB. When UFB are generated, they tend to shrink underwater due to the rapid dissolution of their internal gas and the pressurized conditions. This dissolution is due to the high surface area to volume ratio, whereas surface tension is responsible for creating pressurized conditions (Agarwal et al., 2011; Gurung et al., 2016; Takahashi et al., 2021).

It is also well established that the gas–water interfaces are negatively charged over a wide pH range, which results in an increased zeta potential of the UFB, which can indicate excessive accumulation of adsorbed ions (mainly hydroxyl ions; Takahashi, 2005; Takahashi et al., 2007; Takahashi et al., 2021). The complete dissolution of the internal gas in the UFB can result in the disappearance of the gas–water interface, which can in turn activate radical generation by scattering the increased electric potential that accumulated due to the adsorbed ions at the interface (Agarwal et al., 2011; Li et al., 2009; Takahashi et al., 2007). In this study the overall increased log reductions in fresh and aged *L. monocytogenes* biofilms on polypropylene, silicone, and stainless surfaces with the incorporation of air, CO_2 , and N_2 UFB may be attributed to the accelerated accumulation of hydroxide ions and subsequent higher generation of hydroxyl radical ions.

The increased AM potency with the addition of UFB on biofilms has been successfully demonstrated by several studies, including the use of UFB alone or in combination with neutral electrolyzed water for removing *E. coli* O157:H7, *Vibrio parahaemolyticus*, and *L. innocua* biofilms on plastic and stainless steel coupons (Shiroodi et al., 2021), inactivation of *Pseudomonas aeruginosa*, and *Staphylococcus aureus* biofilms by using laser induced vapor UFB (Teirlinck et al., 2019), and the removal of *P. aeruginosa* biofilms on stainless steel and polypropylene surfaces as well as carbohydrate, protein, and fat removal from stainless steel using UFB (Burfoot et al., 2017).

The increased log reductions in fresh and aged *L. monocytogenes* biofilms using CO_2 UFB compared with the other gas used to make UFB could be attributed to the ability of CO_2 to form carbonic acid in aqueous solutions; hence, increasing the ability of the AMs to penetrate through the microbial cell's membrane (Martirosyan et al., 2012). Martirosyan et al. (2012) evaluated CO_2 in combination with calcium hypochlorite against *E. coli* K-12 in water purification and determined that CO_2 could penetrate the microbial cells easily, hence increasing the efficacy of calcium hypochlorite's toxic effect on the microbial cells. Similarly, supercritical CO_2 was evaluated in combination with PAA against *E. coli* and *L. innocua* by Sikin et al. (2017), and they concluded that CO_2 acted as a vector for PAA to easily penetrate and inactivate the microbial cells. Similar results were observed in a previous study conducted by Sekhon et al. (2021), in which the incorporation of CO_2 UFB in 100 ppm Cl_2 led to significantly greater log reductions in *L. monocytogenes* biofilms on stainless steel surfaces compared with 100 ppm Cl_2 without UFB.

The Eh of any AM solutions can depend on various factors including, type and concentration of AM, temperature and pH of the solution, dissolved air/oxygen, and presence of organic matter in the solution (Lie & Welander, 1994; Wu & Wang, 2012; Yuan et al., 2013). Even though there is no direct connection between pH and Eh, a decline in pH usually results in an uprise in Eh, and vice versa (Morris, 2000).

Carbon dioxide's ability to form carbonic acid in aqueous solutions could also contribute to the significantly lower pH observed in the CO_2 UFB solutions. Singh et al. (2021) demonstrated similar results when evaluating the incorporation of air, CO_2 , and N_2 , MNBs on the efficacy of commonly used AMs in the food industry against pure cultures of *E. coli* O157:H7 and *L. monocytogenes*. Debs-Louka et al. (1999) when employed compressed CO_2 to evaluate its effect against *E. coli*, *Saccharomyces cerevisiae*, and *Enterococcus faecalis* in a solid hydrophilic medium and concluded that the decreased pH of the medium was attributed to the production of carbonic acid.

In summary, this study demonstrated that the incorporation of air, CO_2 , and N_2 UFB in Cl_2 (50, 100, and 200 ppm) and PAA (20, 40, and 80 ppm) solutions resulted in significantly greater log reductions in fresh and aged *L. monocytogenes* biofilms on polypropylene and stainless steel surfaces compared with AMs without UFB. Also, the incorporation of CO_2 UFB in AM solutions resulted in greater reduction in fresh and aged *L. monocytogenes* biofilms on silicone surfaces. This study also demonstrated that the application of 200 ppm Cl_2 resulted in significantly greater log reductions in fresh and aged *L. monocytogenes* biofilms on polypropylene, silicone, and stainless steel surfaces compared with 50 ppm Cl_2 , 20 ppm PAA, and 40 ppm PAA. Due to pathogens responding differently to different AMs and concentrations, individual pathogens should be tested for various UFB AM solutions. Similarly, with vast difference in surfaces textures and composition, individual surfaces should be tested for effectiveness of various UFB AM solutions against biofilms. Eventually, incorporation of UFB should also be studied for the use of wash AM solutions in the fresh produce and meat industry.

FUNDING INFORMATION

This research was funded by the BUILD Dairy program of the Western Dairy Center, Logan, Utah, USA.

CONFLICT OF INTEREST STATEMENT

The authors have no conflict of interest to declare.

DATA AVAILABILITY STATEMENT

The data that support the findings of this study are available from the corresponding author upon reasonable request.

ORCID

Minto Michael  <https://orcid.org/0000-0002-4625-8061>

REFERENCES

- Agarwal, A., Ng, W. J., & Liu, Y. (2011). Principle and applications of micro-bubble and nanobubble technology for water treatment. *Chemosphere (Oxford)*, 84(9), 1175–1180. <https://doi.org/10.1016/j.chemosphere.2011.05.054>
- Ahmed, A. K. A., Shi, X., Hua, L., Manzueta, L., Qing, W., Marhaba, T., & Zhang, W. (2018). Influences of air, oxygen, nitrogen, and carbon dioxide nanobubbles on seed germination and plant growth. *Journal of Agricultural and Food Chemistry*, 66(20), 5117–5124. <https://doi.org/10.1021/acs.jafc.8b00333>
- Arumugam, P. (2015). Understanding the fundamental mechanisms of a dynamic micro-bubble generator for water processing and cleaning applications (Thesis). https://tspace.library.utoronto.ca/bitstream/1807/70241/1/Arumugam_Palaniappan_201511_MAS_thesis.pdf.
- Asada, R., Kageyama, K., Tanaka, H., Matsui, H., Kimura, M., Saitoh, Y., & Miwa, N. (2010). Antitumor effects of nano-bubble hydrogen-dissolved water are enhanced by coexistent platinum colloid and the combined hyperthermia with apoptosis-like cell death. *Oncology Reports*, 24(6), 1463–1470. <https://doi.org/10.3892/or.00001006>
- Bourdichon, F., Lindsay, D., Dubois, A., & Jordan, K. (2019). Ecology of *Listeria* spp. and *Listeria monocytogenes*, significance in dairy production. International Dairy Federation (IDF). Retrieved December 11, 2022, from <https://fil-idf.org/publications/bulletin/bulletin-of-the-idf-n-502-2019-ecology-of-listeria-spp-and-listeria-monocytogenes-significance-in-dairy-production/>.
- Bremer, P., Flint, S., Brooks, J., & Palmer, J. (2015). Introduction to biofilms: Definition and basic concepts. In *Biofilms in the dairy industry*. Wiley Blackwell.
- Burfoot, D., Limburn, R., & Busby, R. (2017). Assessing the effects of incorporating bubbles into the water used for cleaning operations relevant to the food industry. *International Journal of Food Science & Technology*, 52(8), 1894–1903. <https://doi.org/10.1111/ijfs.13465>
- Carvalho, F., Sousa, S., & Cabanes, D. (2014). How *Listeria monocytogenes* organizes its surface for virulence. *Frontiers in Cellular and Infection Microbiology*, 4(48), 1–11. <https://doi.org/10.3389/fcimb.2014.00048>
- Centers for Disease Control and Prevention (CDC). (2022a). *Listeria* (Listeriosis). Retrieved December 10, 2022 from <https://www.cdc.gov/listeria/index.html>.
- Centers for Disease Control and Prevention (CDC). (2022b). *Listeria* Outbreaks. Retrieved December 10, 2022 from, <https://www.cdc.gov/listeria/outbreaks/index.html>.
- Chen, J., Luo, X., Jiang, L., Jin, P., Wei, W., Liu, D., & Fang, W. (2009). Molecular characteristics and virulence potential of *Listeria monocytogenes* isolates from Chinese food systems. *Food Microbiology*, 26(1), 103–111. <https://doi.org/10.1016/j.fm.2008.08.003>
- Cornell University. (2008). *Listeria monocytogenes* in the dairy environment. Retrieved December 10, 2022, from <https://foodsafety.foodscience.cornell.edu/sites/foodsafety.foodscience.cornell.edu/files/shared/documents/CU-DFScience-Notes-Listeria-EnvironControl-01-08.pdf>.
- Debs-Louka, E., Louka, N., Abraham, G., Chabot, V., & Allaf, K. (1999). Effect of compressed carbon dioxide on microbial cell viability. *Applied and Environmental Microbiology*, 65(2), 626–631. <https://doi.org/10.1128/AEM.65.2.626-631.1999>
- Demangeat, J. L. (2015). Gas nanobubbles and aqueous nanostructures: The crucial role of dynamization. *Homeopathy*, 104(2), 101–115. <https://doi.org/10.1016/j.homp.2015.02.001>
- Dhungana, P., & Bhandari, B. (2021). Development of a continuous membrane nanobubble generation method applicable in liquid food processing. *International Journal of Food Science & Technology*, 56(9), 4268–4277. <https://doi.org/10.1111/ijfs.15182>
- Flemming, H. C., Baveye, P., Neu, T. R., Stoodley, P., Szewzyk, U., Wingender, J., & Wuertz, S. (2021). Who put the film in biofilm? The migration of a term from wastewater engineering to medicine and beyond. *Biofilms and Microbiomes*, 7(1), 1–5. <https://doi.org/10.1038/s41522-020-00183-3>
- Flemming, H. C., & Wingender, J. (2010). The biofilm matrix. *Nature Reviews. Microbiology*, 8(9), 623–633. <https://doi.org/10.1038/nrmicro2415>
- Flemming, H. C., Wingender, J., Szewzyk, U., Steinberg, P., Rice, S. A., & Kjelleberg, S. (2016). Biofilms: An emergent form of bacterial life. *Nature Reviews. Microbiology*, 14(9), 563–575. <https://doi.org/10.1038/nrmicro.2016.94>
- Ghadimkhani, A., Zhang, W., & Marhaba, T. (2016). Ceramic membrane defouling (cleaning) by air Nano bubbles. *Chemosphere (Oxford)*, 146, 379–384. <https://doi.org/10.1016/j.chemosphere.2015.12.023>
- Guo, Z., Wang, X., Wang, H., Hu, B., Lei, Z., Kobayashi, M., Adachi, Y., Shimizu, K., & Zhang, Z. (2019). Effects of nanobubble water on the growth of 1028 and its lactic acid production. *RSC Advances*, 9(53), 30760–30767. <https://doi.org/10.1039/c9ra05868k>
- Gurung, A., Dahl, O., & Jansson, K. (2016). The fundamental phenomena of nanobubbles and their behavior in wastewater treatment technologies. *Geosystem Engineering*, 19(3), 133–142. <https://doi.org/10.1080/12269328.2016.1153987>
- Hayakumo, S., Arakawa, S., Takahashi, M., Kondo, K., Mano, Y., & Izumi, Y. (2014). Effects of ozone nano-bubble water on periodontopathic bacteria and oral cells - In vitro studies. *Science and Technology of Advanced Materials*, 15(5), 55003–55007. <https://doi.org/10.1088/1468-6996/15/5/055003>
- Horejs, C. M. (2018). Bubbly for bacteria. *Nature Review Materials*, 3, 457. <https://doi.org/10.1038/s41578-018-0068-x>
- International Organization for Standardization (ISO). (2017). Fine bubble technology – General principles for usage and measurement of fine bubbles— Part 1: Terminology. Retrieved December 12, 2022, from <https://www.iso.org/obp/ui/#iso:std:iso:20480:-1:ed-1:v1:en>.
- Khalesi, M., Gebruers, K., Riveros-Galan, D., Deckers, S., Moosavi-Movahedi, A. A., Verachtert, H., & Derdelinckx, G. (2016). Hydrophobic purification based on the theory of CO₂-nanobubbles. *Journal of Liquid Chromatography & Related Technologies*, 39(3), 111–118. <https://doi.org/10.1080/10826076.2015.1132725>
- Li, P., Takahashi, M., & Chiba, K. (2009). Enhanced free-radical generation by shrinking microbubbles using a copper catalyst. *Chemosphere (Oxford)*, 77(8), 1157–1160. <https://doi.org/10.1016/j.chemosphere.2009.07.062>
- Lie, E., & Welander, T. (1994). Influence of dissolved oxygen and oxidation–reduction potential on the denitrification rate of activated sludge. *Water Science and Technology*, 30(6), 91–100. <https://doi.org/10.2166/wst.1994.0256>
- Liu, S., Oshita, S., Kawabata, S., Makino, Y., & Yoshimoto, T. (2016). Identification of ROS produced by nanobubbles and their positive and negative effects on vegetable seed germination. *Langmuir*, 32(43), 11295–11302. <https://doi.org/10.1021/acs.langmuir.6b01621>

- Liu, S., Oshita, S., Kawabata, S., & Thuyet, D. Q. (2017). Nanobubble Water's promotion effect of barley (*Hordeum vulgare* L.) sprouts supported by RNA-Seq analysis. *Langmuir*, 33(43), 12478–12486. <https://doi.org/10.1021/acs.langmuir.7b02290>
- Liu, S., Oshita, S., & Makino, Y. (2014). Stimulating effect of nanobubbles on the reactive oxygen species generation inside barley seeds as studied by the microscope spectrophotometer. In International Conference of Agricultural Engineering, Zürich, Germany. (Vol. 6, pp. 1–8).
- Liu, S., Oshita, S., Makino, Y., Wang, Q., Kawagoe, Y., & Uchida, T. (2016). Oxidative capacity of nanobubbles and its effect on seed germination. *ACS Sustainable Chemistry & Engineering*, 4(3), 1347–1353. <https://doi.org/10.1021/acssuschemeng.5b01368>
- Martirosyan, V., Hovnanyan, K., & Ayrapetyan, S. (2012). Carbon dioxide as a microbial toxicity enhancer of some antibacterial agents: A new potential water purification tool. *Biophysics*, 2012, 1–7. <https://doi.org/10.5402/2012/906761>
- Matle, I., Mbatha, K. R., & Madoroba, E. (2020). A review of *Listeria monocytogenes* from meat and meat products: Epidemiology, virulence factors, antimicrobial resistance and diagnosis. *Onderstepoort Journal of Veterinary Research*, 87(1), e1–e20. <https://doi.org/10.4102/ojvr.v87i1.1869>
- Morris, J. G. (2000). The effect of redox potential. *The Microbiological Safety and Quality of Food*, 298(1), 235–250.
- Osek, J., Lachtara, B., & Wieczorek, K. (2022). *Listeria monocytogenes* in foods—From culture identification to whole-genome characteristics. *Food Science & Nutrition*, 10(9), 2825–2854. <https://doi.org/10.1002/fsn3.2910>
- Owen, J., McEwan, C., Nesbitt, H., Bovornchutichai, P., Averde, R., Borden, M., McHale, A. P., Callan, J. F., & Stride, E. (2016). Reducing tumour hypoxia via oral administration of oxygen nanobubbles. *Public Library of Science One*, 11(12), e0168088. <https://doi.org/10.1371/journal.pone.0168088>
- Phan, K., Truong, T., Wang, Y., & Bhandari, B. (2020). Nanobubbles: Fundamental characteristics and applications in food processing. *Trends in Food Science & Technology*, 95, 118–130. <https://doi.org/10.1016/j.tifs.2019.11.019>
- Phan, K., Truong, T., Wang, Y., & Bhandari, B. (2021). Effect of electrolytes and surfactants on generation and longevity of carbon dioxide nanobubbles. *Food Chemistry*, 363, 130299. <https://doi.org/10.1016/j.foodchem.2021.130299>
- Scallan, E., Hoekstra, R. M., Angulo, F. J., Tauxe, R. V., Widdowson, M.-A., Roy, S. L., Jones, J. L., & Griffin, P. M. (2011). Foodborne illness acquired in the United States—Major pathogens. *Emerging Infectious Diseases*, 17(1), 7–15. <https://doi.org/10.3201/eid1701.P11101>
- Sekhon, A. S., Unger, P., Singh, A., Yang, Y., & Michael, M. (2021). Impact of gas ultrafine bubbles on the potency of chlorine solutions against *Listeria monocytogenes* biofilms. *Journal of Food Safety*, 42, e12954. <https://doi.org/10.1111/jfs.12954>
- Shiroodi, S., Schwarz, M. H., Nitin, N., & Ovissipour, R. (2021). Efficacy of Nanobubbles alone or in combination with neutral electrolyzed water in removing *Escherichia coli* O157:H7, *Vibrio parahaemolyticus*, and *Listeria innocua* biofilms. *Food and Bioprocess Technology*, 14(2), 287–297. <https://doi.org/10.1007/s11947-020-02572-0>
- Sikin, A. M., Walkling-Ribeiro, M., & Rizvi, S. S. H. (2017). Synergistic processing of skim milk with high pressure nitrous oxide, heat, Nisin, and lysozyme to inactivate vegetative and spore-forming bacteria. *Food and Bioprocess Technology*, 10(12), 2132–2145. <https://doi.org/10.1007/s11947-017-1982-4>
- Singh, A., Sekhon, A. S., Unger, P., Babb, M., Yang, Y., & Michael, M. (2021). Impact of gas micro-nano-bubbles on the efficacy of commonly used antimicrobials in the food industry. *Journal of Applied Microbiology*, 130(4), 1092–1105. <https://doi.org/10.1111/jam.14840>
- Takahashi, M. (2005). ζ potential of microbubbles in aqueous solutions: Electrical properties of the gas-water Interface. *The Journal of Physical Chemistry. B*, 109(46), 21858–21864. <https://doi.org/10.1021/jp0445270>
- Takahashi, M., Chiba, K., & Li, P. (2007). Free-radical generation from collapsing microbubbles in the absence of a dynamic stimulus. *The Journal of Physical Chemistry. B*, 111(6), 1343–1347. <https://doi.org/10.1021/jp0669254>
- Takahashi, M., Shirai, Y., & Sugawa, S. (2021). Free-radical generation from bulk Nanobubbles in aqueous electrolyte solutions: ESR spin-trap observation of microbubble-treated water. *Langmuir*, 37(16), 5005–5011. <https://doi.org/10.1021/acs.langmuir.1c00469>
- Teirlinck, E., Fraire, J. C., Van Acker, H., Wille, J., Swimberghe, R., Brans, T., Xiong, R., Meire, M., De Moor, R. J. G., De Smedt, S. C., Coenye, T., & Braeckmans, K. (2019). Laser-induced vapor nanobubbles improve diffusion in biofilms of antimicrobial agents for wound care. *Biofilm*, 1, 100004. <https://doi.org/10.1016/j.biofilm.2019.100004>
- Thurnheer, T., Gmur, R., Shapiro, S., & Guggenheim, B. (2003). Mass transport of macromolecules within an in vitro model of supragingival plaque. *Applied and Environmental Microbiology*, 69, 1702–1709. <https://doi.org/10.1128/AEM.69.3.1702-1709.2003>
- Tvrđá, E., & Benko, F. (2020). Free radicals: what they are and what they do. *Pathology*, 3–13. <https://doi.org/10.1016/b978-0-12-815972-9.00001-9>
- U.S. Food and Drug Administration (FDA). (2022). *Listeria* (Listeriosis). U.S. Food and Drug Administration. Retrieved December 10, 2022, from <https://www.fda.gov/food/foodborne-pathogens/listeria-listeriosis>.
- Ushikubo, F. Y., Furukawa, T., Nakagawa, R., Enari, M., Makino, Y., Kawagoe, Y., Shiina, T., & Oshita, S. (2010). Evidence of the existence and the stability of nano-bubbles in water. *Colloids and Surfaces: A Physicochemical and Engineering Aspects*, 361(1), 31–37. <https://doi.org/10.1016/j.colsurfa.2010.03.005>
- Vert, M., Doi, Y., Hellwich, K., Hess, M., Hodge, P., Kubisa, P., Rinaudo, M., & Schué, F. (2012). Terminology for biorelated polymers and applications (IUPAC recommendations 2012). *Pure and Applied Chemistry*, 84(2), 377–410. <https://doi.org/10.1351/PAC-REC-10-12-04>
- Wu, H., & Wang, S. (2012). Impacts of operating parameters on oxidation–Reduction potential and pretreatment efficacy in the pretreatment of printing and dyeing wastewater by Fenton process. *Journal of Hazardous Materials*, 243, 86–94. <https://doi.org/10.1016/j.jhazmat.2012.10.030>
- Yuan, H., Nie, J., Zhu, N., Miao, C., & Lu, N. (2013). Effect of temperature on the wastewater treatment of a novel anti-clogging soil infiltration system. *Ecological Engineering*, 57, 375–379. <https://doi.org/10.1016/j.ecoleng.2013.04.007>

How to cite this article: Unger, P., Sekhon, A. S., Sharma, S., Lampien, A., & Michael, M. (2023). Impact of gas ultrafine bubbles on the efficacy of antimicrobials for eliminating fresh and aged *Listeria monocytogenes* biofilms on dairy processing surfaces. *Journal of Food Safety*, e13057. <https://doi.org/10.1111/jfs.13057>